CHAPTER 5

Rotor Impact Mills

Roland Nied*

Dr. Nied Consulting, Raiffeisenstraße 10, 86486 Bonstetten, Germany

Contents

Abstract

The stress in rotor impact mills is characterised by impact processes in the rotor and in the milling gap. A distinction can be made between particle impacts with the impact beaters, particle–particle impacts in the milling gap and particle–stator impacts.

The main influences on the milling result are produced by the rotor circumferential speed, the particle acceleration in the rotor and the conditions in the milling gap.

The fineness of the milled material can be significantly influenced amongst other things by the impact frequency. Integrated classification in particular is a suitable means of selectively increasing the impact frequency for the large particles due to the longer dwell time.

By means of the model presentation and empirical values, rules will be developed for the scaling-up of rotor impact mills.

Finally, the most important designs will be described, such as universal mills, pin disc mills and classifier mills.

*Corresponding author. Tel.: +49-8293-6756; Fax: +49-8293-7136;
E-mail: Roland.Nied@drnied.de

Handbook of Powder Technology, Volume 12
ISSN 0167-3785, DOI: 10.1016/S0167-3785(07)12008-X

1. INTRODUCTION

The term *rotor impact mills* refers to crushing machines, in which the crushing is carried out by impact stresses, and the kinetic energy (impact energy) required to produce the impact stress is applied by the rotary movement of rotors.

Rotor impact mills cover a wide fineness range, which extends from a final particle size in the area of a few millimetres, down to less than about 10 μm. In the coarser range, rotor impact mills are frequently referred to as crushers (hammer-crushers) and in the finer range as blast rotor mills, wing beater mills, pin disc mills etc.

The common feature of all rotor impact mills is the usually centrally arranged rotor, which is equipped with tools of different shapes. Static milling elements can be arranged concentrically around the rotor. Classification of the milled material can be achieved by means of grills, screens or integrated classifiers.

The main area of application of rotor impact mills is the crushing of brittle materials with a Mohs-hardness of up to 3. Cold milling processes are available for special purposes (milling of plastics, spices etc.). The air is usually warmed for drying during the milling process. Further special versions include the pressure shock resistant, gas-tight (for circulating gas operation) or sterilisable design.

Rotor impact mills represent a universally used type of mill. The following systematic description of rotor impact mills cannot claim to be comprehensive, in view of the wide existing variety, so that only little space is devoted, for example, to pin disc mills. The article deals essentially with rotor impact mills using impact beaters as the rotating tools, for which the most comprehensive research results are also available.

2. MODEL OF THE MILLING PROCESS IN ROTOR IMPACT MILLS

The most common form of rotor impact mills makes use of plate-shaped milling tools on the rotor, with a central milling material feed into the interior of the rotor (Fig. 1).

The milling material, together with the air, which is carried along by the centrifugal force in the rotor, is fed through the inlet pipe (1) arranged centrally with the rotor (2) and is carried by the air into the area of the impact beaters (3). The crushing is carried out by impacts with the beaters and other particles in the milling gap (4) or with the stator (5).

For the impact of one particle against another or against a surface, the following types of impacts can be distinguished ([1], Fig. 2):

- Direct impact, the angle between the direction of impact and the direction of movement is zero.

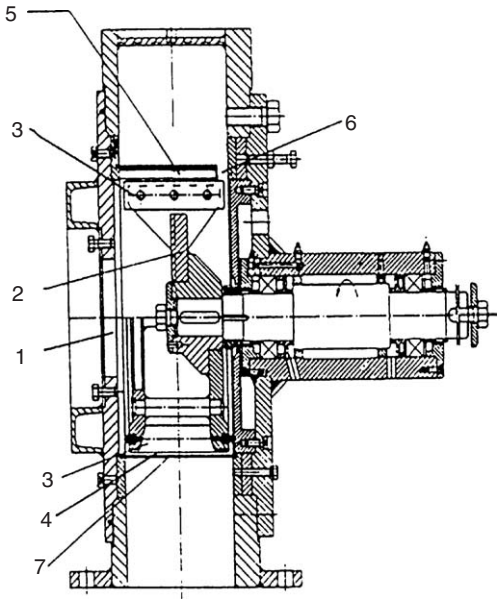

Fig. 1. Section through a rotor impact mill with plate-shaped milling elements: 1, milling material feed; 2, rotor; 3, plate-shaped milling element (*impact beater*); 4, milling gap; 5, stator (*grinding track*) with outlet gap 6; 7, alternative stator (*screen*) with outlet through the screen perforation.

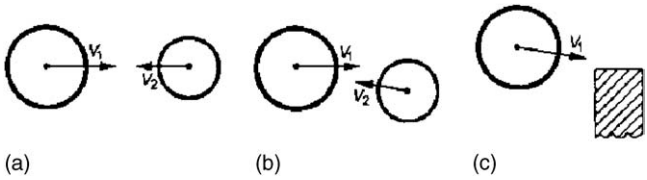

Fig. 2. Impact types to [1]: (a): direct impact; (b) angular impact; (c) edge impact.

- Angular impact, the angle between the direction of impact and the direction of movement differs from zero; this type also includes direct eccentric impact.
- Edging impact, in which the centre of the particle lies outside the surface volume.

The highest level of energy transfer usable in the crushing process is achieved in the case of direct impact; in the case of angular or edge impact, rotation or slippage also occurs.

In addition to the type of impact, the point of application of the stress also largely determines the milling result. In rotor impact mills, there are two main

stress points:

- Impact processes on the broad side and the edges of the impact beaters (in the rotor) and
- Impact processes in the milling gap and at the stator.

2.1. Impact processes in the rotor

As already described, the milling material enters the interior of the rotor together with the milling gas transported by the mill. The radial acceleration of the particles, apart from wall influences, is provided by the drag force of the milling gas; the particle movement is essentially radial [2,3]. Provided that the particles in the interior of the rotor are evenly distributed, and that their radial speed corresponds to the radial speed of the milling gas, their penetration depth h between the impact beaters can be estimated (Fig. 3).

A group of particles of approximately h_{max} s_i moves radially outward at the speed v_P. At the same time, the impact beaters ''1'' and ''2'' move at the circumferential speed w_i. The particles of the group which first passes the side opposed to the movement direction of impact rail ''1'' achieves the greatest penetration depth h_{max}. The particle which is simultaneously at the position $R_i - h_{max}$, achieves the lowest penetration depth $h = 0$. If the time window needed by the impact rail ''2'' for traversing the distance s_i and the radial speed of the group of particles are known, the penetration depth h can be calculated. We first calculate the time required by the impact beater ''2'' to traverse the distance s_i:

$$t = s_i / w_i \tag{1}$$

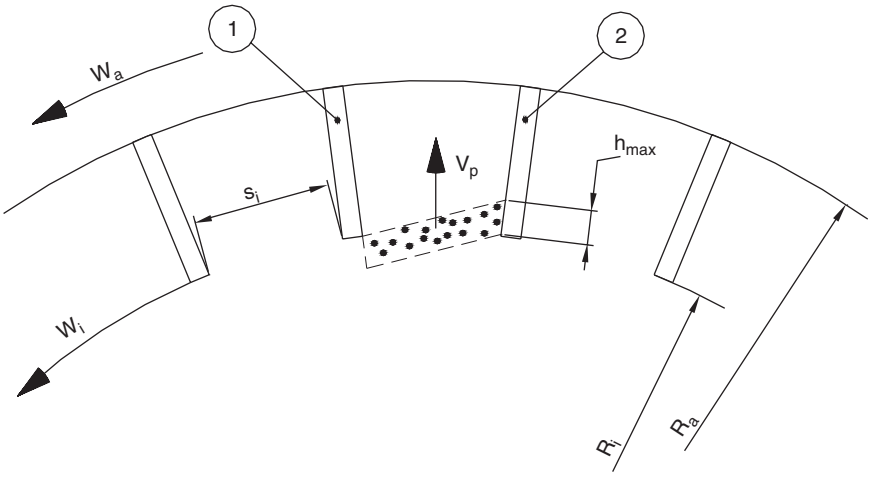

Fig. 3. Model of the penetration depth h between the impact beaters of a rotor impact mill.

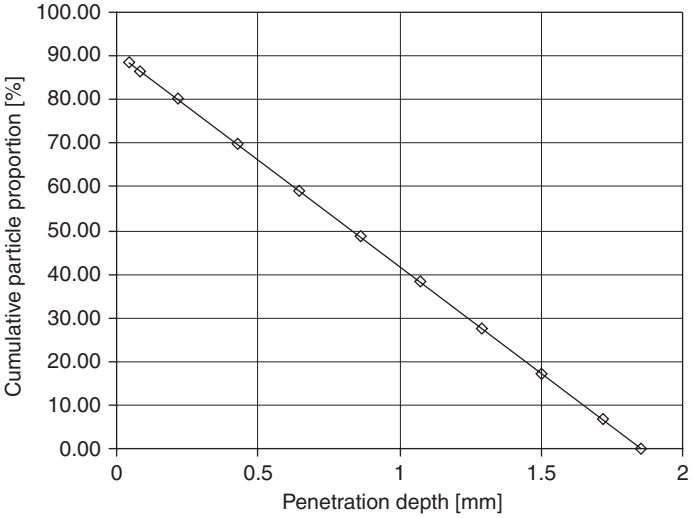

Fig. 4. Cumulative proportion of particles which reach a particular penetration depth.

During this time, the particle $h = h_{max}$ moves by the distance

$$h_{max} = tv_p \tag{2}$$

into the impact circle. All other particles of the group have a shorter time available for their radial penetration into the impact circle. If we calculate the penetration depth for different points in time t, we obtain a cumulative proportion of particles which achieve a particular penetration depth up to $h = h_{max}$.

Figure 4 graphically interprets the result of such an estimate for a rotor impact mill with a rotor external diameter of 300 mm ($v_P = 4.3$ m/s, $w_i = 73$ m/s, $s_i = 28.4$ mm, free surface area between the impact rails 90.5%).

A particle which penetrates into the impact circle immediately after passing the impact beater ''1'' therefore achieves a maximum penetration depth of 1.85 mm. The later the particle enters, the lower the penetration depth. To this is added a proportion of particles which do not penetrate into the impact circle: this corresponds to the total of the impact rail surface area facing the interior of the rotor, divided by the total surface area (in this example 9.5%).

The typical particle diameter for the feed material in rotor impact mills lies in the range from 1 mm up to several millimetres. In order to estimate the type of impact to which the particles are subjected, we will assume a particle radius of 1 mm. A surface impact only occurs in the case of particles which achieve a penetration depth greater than 1 mm (in this example about 40%). If the penetration depth is less than 1 mm, the particles undergo an edge impact. Pieces and uncrushed particles are transported back into the interior of the rotor at a speed increased by a factor of about 10 ([2], Fig. 5). This increased speed now enables them to

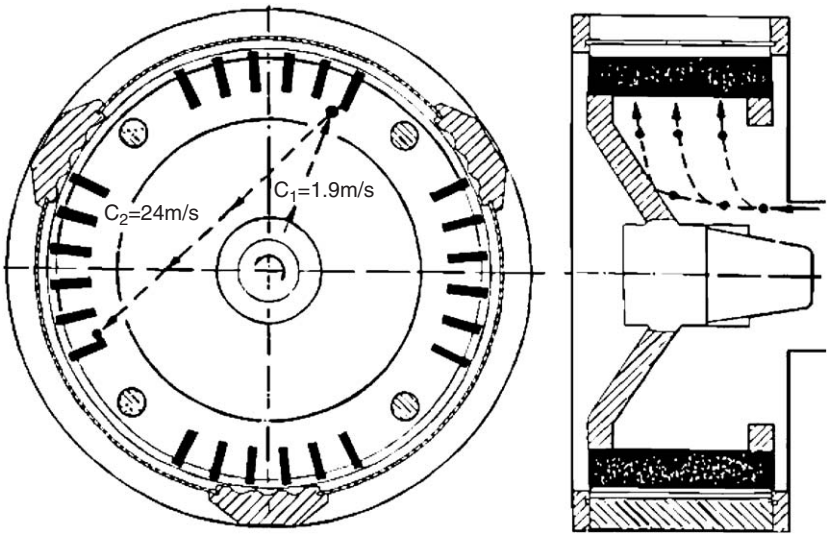

Fig. 5. Rotor impact mill with screen and milling jaws showing the particle movement in the inlet, together with the speed c_1 prior to the 1st impact and c_2 after the 1st impact (from [2]). Rotor circumferential speed 40 m/s.

penetrate between the impact beaters, where they are also subjected to a surface impact, before being accelerated along the broad side of the impact rail [2].

Using the following assumptions:

- friction-free particle movement
- acceleration path = width of impact rails = $R_a - R_i$
- radial speed of particles prior to impact $v_{P,i} = 0$

we can derive the movement equation for the acceleration process as follows:

$$b_r = dv_P/dt = dv_P/dR\, dR/dt = dv_P/dR\, v_P \tag{3}$$

$$b_r = \omega^2 R \tag{4}$$

$$\Rightarrow \omega^2 R\, dR = v_P dv_P \tag{5}$$

By integration within the limits R_i and R_a and with $\omega = w_{R,a}/R_a$ we obtain

$$v_{P,a} = w_{R,a}(1 - R_i^2/R_a^2)^{0.5} \tag{6}$$

Under the further assumption that the particle circumferential speed $w_{P,a}$ equals the impact beaters circumferential speed $w_{R,a}$, the particle ejection speed c_P can be expressed as

$$c_P = w_{R,a}(2 - R_i^2/R_a^2)^{0.5} \tag{7}$$

It can easily be seen that for $R_i \Rightarrow 0$ (i.e. impact beater width $B = R_a$) and friction-free consideration the particle ejection speed c_p lies above the rotor circumferential speed $w_{R,a}$ by the factor $\sqrt{2}$ [3].

The particle ejection angle can finally be calculated as

$$\beta = \arctan(v_{P,a}/w_{P,a}) \tag{8}$$

2.2. Impact processes in the milling gap

Following the acceleration process, the particles enter the ring-shaped area between the impact beaters and the stator. In this milling gap, the milling material rotates in a cloud. The average free path length λ and the particle braking path s_0 in the milling gap can be estimated ([4], Fig. 6). Depending on the volume concentration $1 - \varepsilon$ and the particle speed c_P, which is correlated with the rotor circumferential speed $w_{R,a}$ in accordance with the equation (7), the following areas can be distinguished for a typical milling gap s of from 2 to 8 mm:

- For particles > 1 mm is $\lambda > s$, $s_0 \gg s$. Mutual particle impacts in the milling gap are unlikely. The impact on the stator takes place at almost unchanged speed.

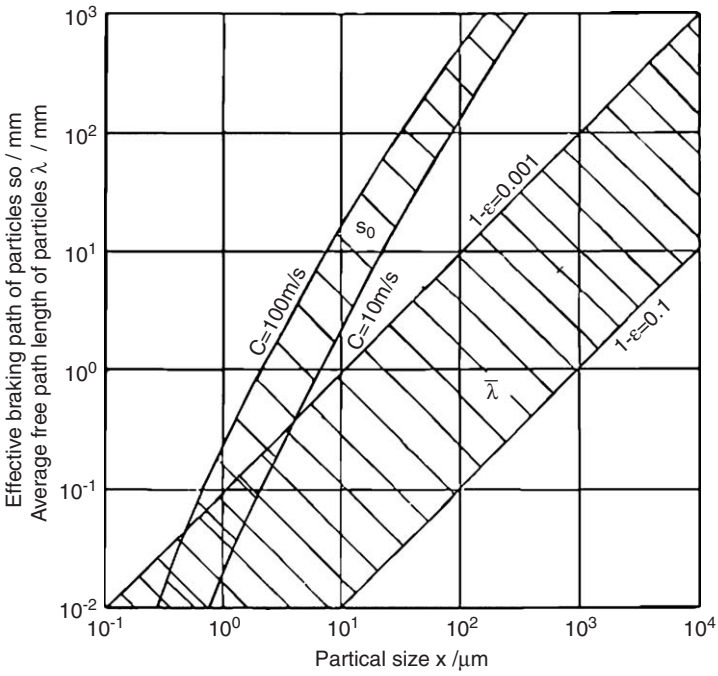

Fig. 6. Free path length and braking path s_o of spherical particles ($\rho = 10^3$ kg/m^3) in stationary air from [4]. Starting speed of particles 10 – 100 m/s; Volume concentration of the milling material in the milling gap $1-\varepsilon =$ 0.1 – 0.001.

- In the size range from 100 µm to 1 mm is $\lambda \approx S$, $s_0 \geq s$. Both particle–particle impacts and impacts on the stator occur. The influence of the particle braking as a result of the flight path is negligible.
- For particle sizes between 10 µm and 100 µm is $\lambda \approx$ s, $s_0 \gg s$. The particle–particle impacts in the milling gap predominate, the braking path s_0 can fall to the order of size of the milling gap s. In this range, the parameters volume concentration 1–ε , size of the milling gap s and the particle speed c_P are very important.
- For particles below 5 µm to 10 µm the stress limits are reached in rotor impact mills. The particle braking path s_0 lies in the range of the milling gap s, and even particle–particle impacts often take place at insufficient speed.
- Finally, for even smaller particles, the braking path s_0 reaches the order of size of the average free path length λ; impact events are no longer probable.

In addition to particle–particle impacts and the impact with the stator, impacts with the outer edges of the impact beaters can also be observed. Particles from the rotating material ring re-enter the area of the impact beaters due to momentum transfer with other particles or with the stator, although in this case, the intensity of the stress is usually lower, since only speed difference between the surrounding ring and the rotor circumferential speed is effective. From [2], the ratio between the particle speed in the surrounding cloud of material in the area of the impact circle and the circumferential speed of the rotor is approximately 0.44 (stator: screen without fittings) to approximately 0.1 (stator: screen with milling jaws; rotor circumferential speed: approximately 43 m/s).

Depending on the fineness range and the selected operating and geometrical parameters, the main impact events taking place are particle–particle or particle–plate impacts. For both cases, the maximum stress force for the central, elastic impact can be estimated according to the Hertz–Huber theory [2,5]:

$$F_{\max} \propto \left(\frac{m_1\, m_2}{m_1 + m_2}\right)^{3/5} \left(\frac{r_1\, r_2}{r_1 + r_2}\right)^{1/5} \left(\frac{1 - v_1}{E_1} + \frac{1 - v_2}{E_2}\right)^{-2/5} c_{\mathrm{rel}}^{6/5} \tag{9}$$

where m is the mass; r the radius; E the elasticity module; and v the contraction number.

The following applies for the impact of a spherical particle with a plate:

$$m_1, r_1, E_1 \ll m_2, r_2, E_2$$

$$F_{\max} \propto m_1^{3/5}\, r_1^{1/5} \left(\frac{1 - v_1}{E_1}\right)^{-2/5} c_{\mathrm{rel}}^{6/5} \tag{10}$$

For the impact of two spherical particles of the same size, this gives:

$$m_1, r_1, E_1 = m_2, r_2, E_2$$

$$F_{max} \propto m_1^{3/5} r_1^{1/5} \left(\frac{1-\nu_1}{E_1}\right)^{-2/5} \left(\frac{c_{rel}}{2}\right)^{6/5} \quad (11)$$

If one compares equations (10) and (11), it can be seen that for the same stress force, the required relative speed in the case of a particle–particle impact must be twice as high as that of a particle–plate impact.

3. CONTROL OF FINENESS

There are three possible procedures (or combinations of these) for the control of fineness in rotor impact mills:

- Influence of the impact type,
- Selection of the stress speed,
- Influence of the impact frequency (dwell time).

3.1. Impact type

The influence of impact type can largely be concluded from the preceding chapter, according to which particle–plate impacts are preferable to particle–particle impacts. Over and above all other considerations therefore, it will have a favourable effect on the achievable fineness, if the volume concentration of the milling material and the milling gap are low.

3.2. Stress speed

In order to initiate rupture, a particle must be supplied with a certain minimum stress energy [2,6]. For the individual impact, the following areas can be distinguished ([1], Fig. 7) for the stress speed, and thus the stress energy:

a. If the stress energy lies below a critical limit, no rupture or crushing will take place, and the energy utilisation is therefore 0.
b. With increasing stress energy, the energy utilisation rises to a maximum value, which corresponds largely to a rupture probability of 100%.
c. After exceeding the optimum stress energy, the energy utilisation declines again.

It will have a favourable influence, both with regard to the energy requirement and the fineness achieved, if the stress speed, and thus also the stress energy are selected so that the energy utilisation is in the area of the optimum.

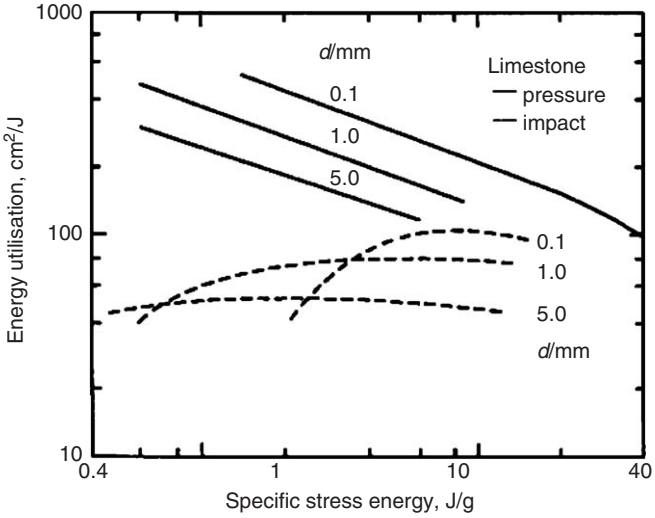

Fig. 7. Energy utilisation of individual particles (limestone) under compression and impact stress [1].

3.3. Influence of impact frequency (dwell time)

If a finer milling result is required, increasing the impact frequency [3,6] can also be considered, in addition to increasing the stress speed. This method can however only be used if the level of the stress speed permits initiation of rupture, i.e. for cases (b) and (c). For the central, direct, elastic impact, the kinetic energy, in the case of multiple impacts multiplied by the impact frequency, can be expressed as

$$E_{\text{kin}} = \frac{m}{2}\, c_{\text{rel}}^2 \tag{12}$$

It can easily be shown that the balanced energy of one individual impact corresponds to that of several impacts at reduced relative speed c_{rel}:

$$E_{\text{kin},1} = \frac{m}{2}\, c_{\text{rel},1}^2 \tag{13}$$

$$n\, E_{\text{kin},2} = n\, \frac{m}{2}\, c_{\text{rel},2}^2 \tag{14}$$

$$E_{\text{kin},1} = n\, E_{\text{kin},2} \tag{15}$$

$$\Rightarrow n = \left(\frac{c_{\text{rel},1}}{c_{\text{rel},2}}\right)^2 \tag{16}$$

(n = number of individual impacts).

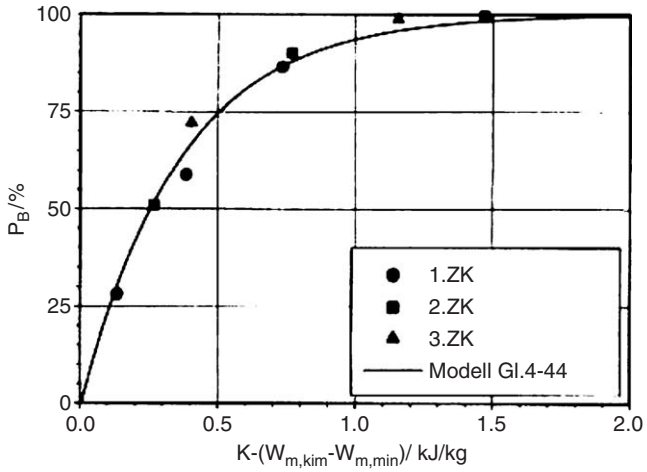

Fig. 8. Probability of rupture of potassium–alum (2 to 2.5 mm, one to three stresses) in relation to the specific impact energy [6].

Figure 8 shows the likelihood of rupture of potassium-alum crystals in relation to the specific impact energy multiplied by the impact frequency [6]. As can be seen, the measured values for one to three stresses all fall along a common curve, representing an experimental confirmation of the relationship derived above.

In order to influence the impact frequency, the dwell time of the milling material in the mill is usually changed, using the following methods:

3.3.1. Non-classifying processes

In rotor impact mills with a profiled grinding track (stator) and an outlet gap (see Fig. 1), the profiling of the grinding track and/or the impact beaters can for example be inclined, in order to produce a conveyor effect away from the outlet gap (Fig. 9).

A further possibility is the use of so-called closed rotors. If one assumes that the milling material is evenly distributed over the length *l* in open blast rotors, the particles that pass the rotor in the vicinity of the outlet gap have only a short dwell time in the milling gap. On the other hand, the particles that pass the rotor at the same height as the inlet are stressed along the whole milling gap length *l* (Fig. 10).

This results in an average effective milling gap length of *l*/2 (and a wide dwell time range). When using a closed rotor, all particles must pass the milling gap along its complete length.

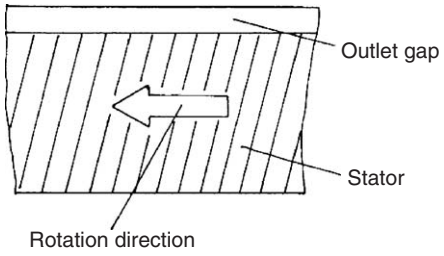

Fig. 9. Schematic representation of a profiled grinding track without classifying effect (plan view).

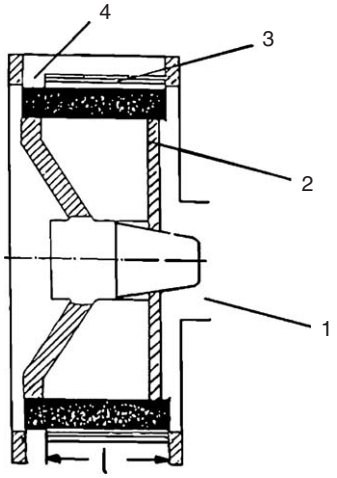

Fig. 10. Section through a rotor impact mill with closed rotor: 1, milling material inlet; 2, closed rotor; 3, grinding track; 4, outlet gap.

The disadvantage with all these procedures is its non-specific effect; even particles which have already attained the required final particle size will be subjected to further impacts, and therefore use up energy unnecessarily. Finally, there is no complete probability of rupture even for coarser particles; instead, quite a wide particle size distribution is generally observed.

3.3.2. Classifying processes

Classifying processes are generally characterised by the fact that only the coarse proportions are subjected to further stress. The fine proportions can leave the mill by suitable means and no longer affect the energy balance. The particle distribution curves of the milled products are therefore generally narrower than in the case of non-classifying processes (no large particles, lower fine proportion). One

possibility of classifying the output consists in the equipment of rotor impact mills with grills or screens. Depending on the angle of incidence of the particles on the screen, the available perforated surface, the perforation dimensions and the thickness (plate thickness) of the screen, the likelihood of penetration can be expressed as a function of the particle size (Fig. 11). Depending on the rotor speed (see Chapter 2, Ejection angle of the accelerated particles from the impact beaters), the volume concentration of the milling material in the milling gap (momentum transfer with other particles) and the air volume flow (air speed at the screen), the angle of incidence will assume different values. In general however, it can be assumed that the resulting particle size will be significantly smaller than the screen perforation used.

The disadvantage of grills or screens as a stator is that profiling of the stator, such as would favour the maximum possible efficiency of the milling, is only possible to a limited extent (see ''Milling jaws'' in Fig. 5). They are also limited in the end fineness that can be achieved: fine screens (approximately $<500\,\mu m$) wear quickly and tend to cause blockage of the screen perforation. Finer milling results (down to approximately $<100\,\mu m$) can however be achieved by special screen designs (e.g. corrugated trapezoid sieves, whose perforations are inclined toward the sieve circumference, and which thus result in a further reduction of the angle of incidence).

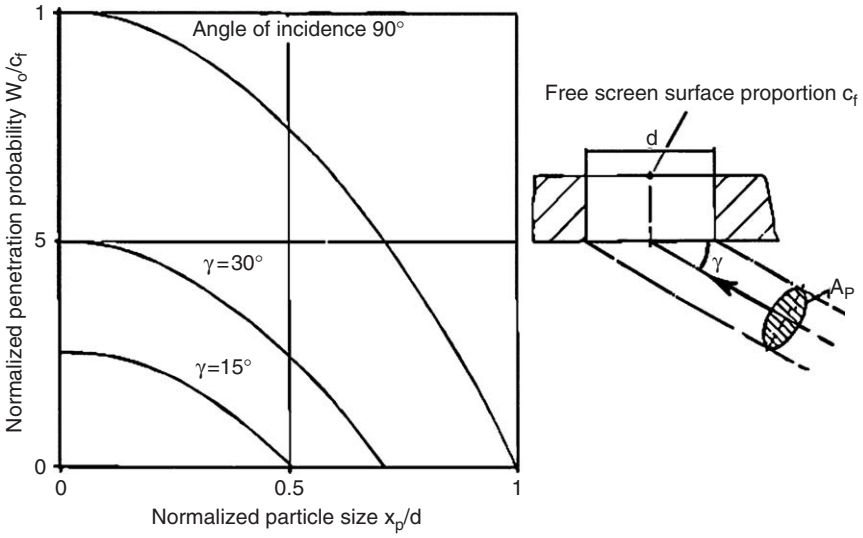

Fig. 11. Penetration probability W_D over the normalised particle size for different angles of incidence from [2]. Thickness of screen not taken into account.

These disadvantages are avoided by rotor impact mills when combined with a classifier[1] to form a so-called classifier mill (see also Fig. 16). The milling material in the mill is transported with the milling air in an inner circuit to the classifier, where the coarse particles are separated from the fine material produced. The fine material leaves the classifier mill together with the milling air. The coarse material, together with the feed material, undergoes further stress.

The separation between milling and classifying enables the rotor and stator to be optimised solely for the task of milling. The fineness of separator mills is limited in the coarse range by the classifier (to approximately 200 μm), and in the fine range by the limits of stress possible in rotor impact mills (to approximately. 10 μm).

4. SCALE-UP

It will only rarely be possible to perform a scale-up without being forced to compromise with regard to individual criteria. In the scaling-up of rotor impact mills, two parameters in particular present difficulties:

1. The working length of the rotor *l*
   If a screen is used as the stator, care must be taken to ensure that the product is distributed evenly along the working length *l*. If the material load becomes too great, this will result in zones of higher stress, particularly on the rear side of the rotor, while the stress will be relatively low in the vicinity of the product inlet.
   When using a grinding track with outlet gap as the stator, the dwell time of the milling material in the milling gap must also be taken into account, which under otherwise similar conditions will depend on the working length *l*. Special importance must be attached to this when using closed rotors.
2. The size of the milling gap *s*
   The milling gap *s* should basically be regarded as a constant in the scaling-up process. Under otherwise similar conditions, the particle-braking path is also constant. If allowed by the production tolerances, this requirement can be fulfilled by using a screen as the stator (in which the through-flow takes place radially).

When using a grinding track as the stator, the through-flow and the product transport take place axially. For the same axial speed in the milling gap, the ring surface $[(R_a + s)^2 - R_a^2]$ must be scaled-up accordingly. The milling gap will then also increase in size in the case of larger mills.

[1] For further information on classification see: R. Nied, Fine classification with vaned rotors, Int. J. Mineral. Process 74S (2004) 137–145.

This needs only to be noted however for very fine milling ($x < 20$–$50\,\mu m$). For $x \geq 50\,\mu m$ the braking path s_o is already about 10 times that of the milling gap s to be expected for larger mills.

The scaling-up model described below has been derived partly empirically, and partly from the models and observations described previously in Section 2. This model assumes the following requirements:

- equal product fineness,
- equal energy utilisation,[2]
- equal ratio of milling material mass flow to milling air volume flow,
- equal circumferential speed at the impact beaters outer edge.

From the point of view of the mill designer, the scale-up factor f is determined as the ratio of the mechanical drive of the mills:

$$f = \frac{P_{M,2}}{P_{M,1}} \tag{17}$$

These requirements give

$$\frac{\dot{m}_2}{\dot{m}_1} = f \tag{18}$$

$$\frac{\dot{V}_2}{\dot{V}_1} = f \tag{19}$$

The further scaling-up is performed by means of the following steps:

a. From experience, one approach has proven itself, which links the radius ratio at the impact beater outer edge with the scale-up factor:

$$\frac{R_{a,2}}{R_{a,1}} = f^{0,6} \tag{20}$$

The exponent of this equation was determined empirically. Manufacturer's data published in the literature [7] demonstrate good conformity with this approach.

Starting from the basic mill, the impact circle radius $R_{a,2}$ can therefore be defined.

b. The impact beaters width $R_a - R_i$ is determined from considerations of the ejection speed and ejection angle (see equation (7) and (8)), according to

[2] Wolf and Pahl [7] found in their investigations of "turbo-mills" with sieve inserts that the energy utilisation was even initially improved following scaling-up, based on a laboratory mill. Constant energy utilisation was then found in the case of larger mills.

which for $w_R = \text{const.}$ the ratio R_i/R_a must be kept constant:

$$\frac{R_{i,1}}{R_{a,1}} = \frac{R_{i,2}}{R_{a,2}} \tag{21}$$

$$\Rightarrow R_{a,2} - R_{i,2} = R_{a,2}\left(1 - \frac{R_{i,1}}{R_{a,1}}\right) \tag{22}$$

c. The impact beaters number n results from the requirement for the same impact beaters distance a at radius R_i (so that the impact and penetration conditions of the particles remain approximately equivalent):

$$a = \frac{2\,R_i\,\pi}{n} = \text{const.} \tag{23}$$

or

$$n = \frac{2\,R_i\,\pi}{a} \tag{24}$$

($a =$ impact beaters distance, $n =$ impact beaters number).

d. In order to achieve similar impact conditions, the total of the impact beaters lengths $n \cdot l$, divided by the material mass flow $\dot{m}$, should be constant (assuming the similarity of the hold-up in the mill):

$$\frac{\dot{m}_2}{n_2\,l_2} = \frac{\dot{m}_1}{n_1\,l_1} \tag{25}$$

$$\Rightarrow l_2 = f \cdot l_1 \cdot \frac{n_1}{n_2} \tag{26}$$

e. The milling gap can be kept approximately constant for rotor impact mills using a screen as the stator (radial through-flow of the milling gap). If a grinding track is used as the stator, the gap width must be determined in accordance with

$$\frac{\dot{V}}{\left[(R_a + s)^2 - R_a^2\right]} = \text{const.} \tag{27}$$

(equal axial flow speed in the milling gap).

5. DESIGNS

The classification of rotor impact mills according to only one feature (e.g. central/tangential milling material feed, with/without classification) is almost impossible:

the known types and designs are too varied. The distinction is therefore often made according to the achievable fineness. Figure 12 shows a possible classification.

The basic features of *hammer mills* (Fig. 13) are the tangential milling material feed and the pendulum-type suspended hammers:

These are generally equipped with the grill and/or screens, and can produce finenesses of approximately. < 1 mm.

Wing beater mills, blast rotor mills and pin disc mills with a rotating disc are today generally classified together as so-called universal mills. These allow the use of different milling tools (rotors and stators) in the same housing (Fig. 14).

The milling material feed for universal mills generally takes place centrally. The rotors are equipped with wing beaters, rigid impact beaters with open (Fig. 14c), semi-closed (Fig. 14b) or closed rotors (see Fig. 10) or also with pins (Fig. 14a). Screens, short grinding track with screen (Fig. 14b), grinding track with outlet gap (Fig. 14c) or again pinned discs are used as the stator. The achievable fineness ranges to a median value of approximately 10 μm.

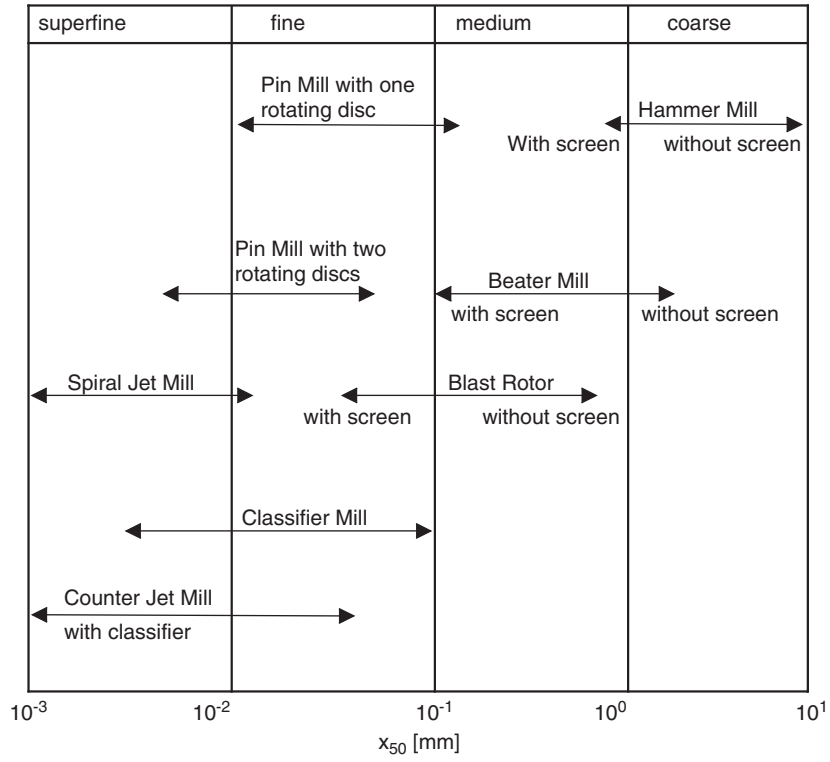

Fig. 12. Fineness range of different impact mills.

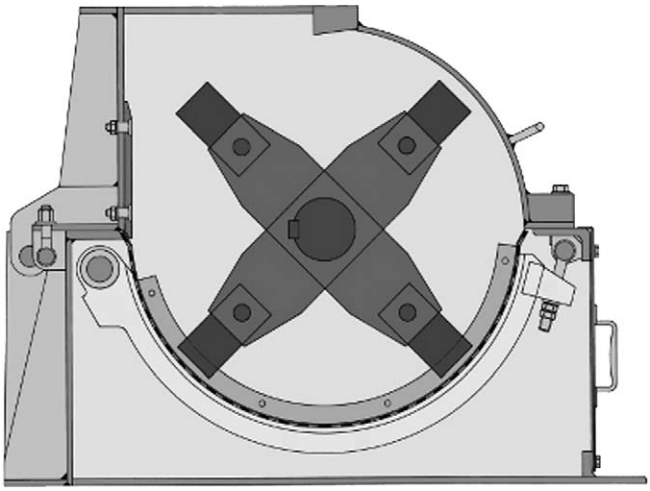

Fig. 13. Schematic representation of a hammer mill. Reproduction with approval of Netzsch–Condux Mahltechnik GmbH, Hanau, Germany.

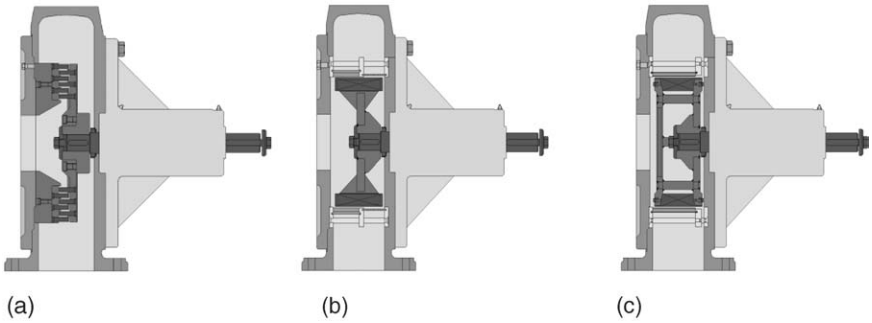

Fig. 14. Schematic representation of a universal mill: (a) rotor: pin disc, stator: pin disc; (b) rotor: wing beaters, stator: short grinding track with screen; (c) rotor: blast rotor, stator: long grinding track with outlet gap. Reproduction with approval of Netzsch–Condux Mahltechnik GmbH, Hanau, Germany.

Pinned disc mills with counter-rotating discs (Fig. 15) achieve the maximum fineness (up to x_{50} 5 μm) amongst rotor impact mills without integrated classifiers.

Thanks to the different rotation directions of the rotors, relative speeds of up to 250 m/s can be achieved at the outer pin rows.

Rotor impact mills with integrated classifiers (see also Section 3.3.2) are frequently referred to as *classifier mills* (Fig. 16).

In the group of rotor impact mills, the maximum finenesses (x_{50} 3 μm) can be achieved by such mills.

Another design worthy of peripheral mention are rotor impact mills with so-called *corrugated-milling discs* (Fig. 17).

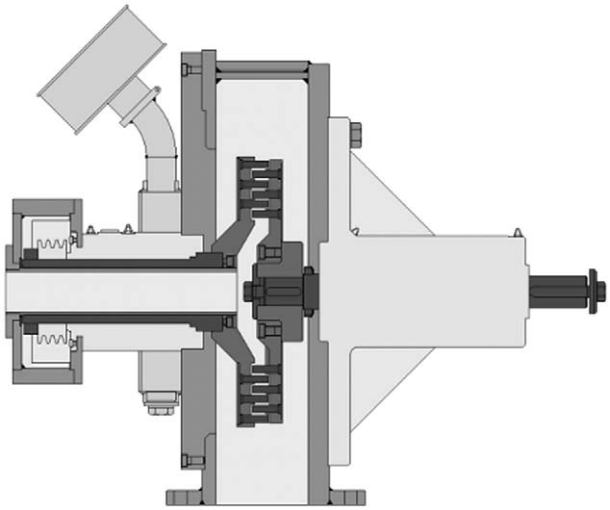

Fig. 15. Section through a counter-rotating pinned disc mill. Reproduction with approval of Netzsch–Condux Mahltechnik GmbH, Hanau, Germany.

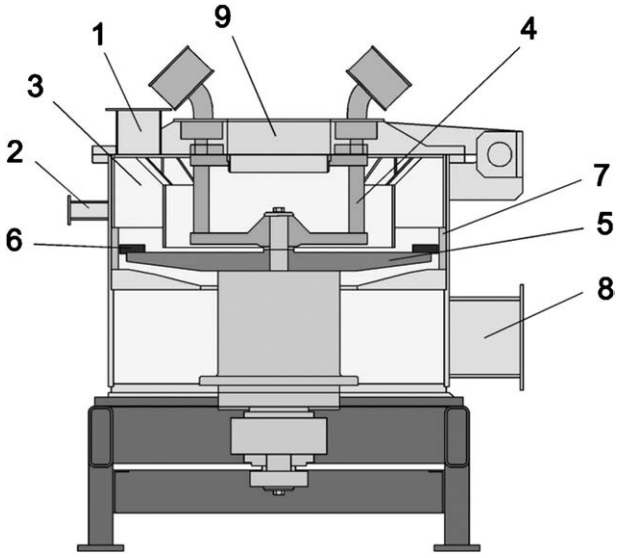

Fig. 16. Section through a classifier mill: 1, 2, milling material feed; 2, 3, Guide vanes; 4, classifier wheel; 5, rotor; 6, impact beaters 7; stator; 8, air inlet; 9, fine material outlet. Reproduction with approval of Netzsch-Condux Mahltechnik GmbH, Hanau, Germany.

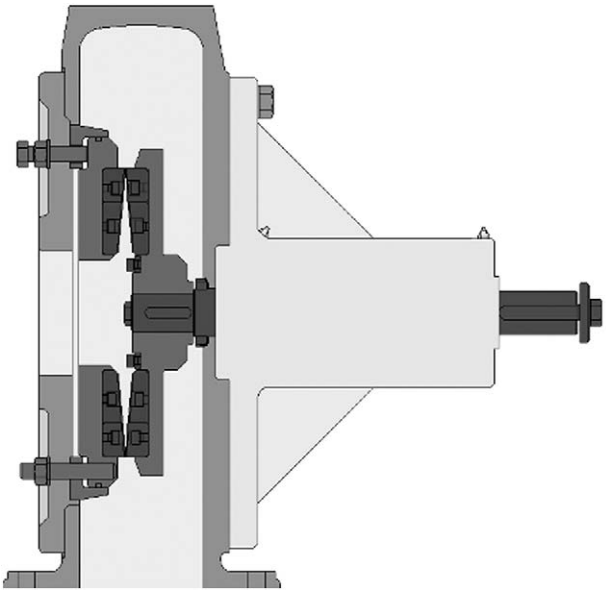

Fig. 17. Schematic representation of a rotor impact mill with ripple-milling discs. Reproduction with approval of Netzsch-Condux Mahltechnik GmbH, Hanau, Germany.

The milling gap can be set very narrow ($s < 1$ mm) with such mills. This favours the additional shear stressing of the milling material, making them ideally suitable for the milling of fibrous, tough elastic materials.

Nomenclature

b_r	radial acceleration (m/s^2)
B	impact rail width (m)
c	speed (m/s)
c_{rel}	relative speed (m/s)
E_A	energy utilisation (m^2/kJ)
E_{kin}	kinetic energy, impact energy (kJ)
f	scaling-up factor (–)
F	stress force (N)
h	penetration depth (m)
l	length of milling gap (m)
m	mass (kg)
$\dot{m}$	mass flow (kg/s)
P	mechanical drive performance (kW)
r	contact radius (m)
R	radius (m)

s_o	particle braking path (mm)
s	path, milling gap width (mm)
t	time (s)
v	radial speed (m/s)
$\dot{V}$	volume flow (m^3/s)
w	circumferential speed (m/s)
x	particle size (μm)
β	particle ejection angle ($^\circ$)
γ	penetration angle ($^\circ$)
ε	porosity (–)
λ	free path length (mm)
ω	angular speed ($^\circ$/s)

Frequently used indices:

a	external
i	internal
P	particle
R	rotor

REFERENCES

[1] K. Schönert, Prallmühlen. Handbuch der Mechanischen Verfahrenstechnik, H. Schubert (Ed.), Wiley-VCH, 2003, pp. 207ff, 355ff.
[2] D. Landwehr, Kaltzerkleinerung in Turbomühlen am Beispiel von Gewürzen, Fortschr.-Ber. VDI Reihe 3, Nr.141, VDI-Verlag, Düsseldorf, 1987.
[3] K. Leschonski, R. Drögemeier, Ultra fine grinding in an impact grinding machine and its limits of application, Australas. Inst. Mining Metall., Publication Series No 3/93, 1 (1993) 227–236.
[4] H. Rumpf, Prinzipien der Prallzerkleinerung und ihre Anwendung bei der Strahlmahlung, CIT 32 (3) (1960) 129–135.
[5] I. Scabo, Höhere Technische Mechanik, Springer Verlag, Berlin, 1977.
[6] L. Vogel, Zur Bruchwahrscheinlichkeit prallbeanspruchter Partikeln, Diss, TU München, 2003, pp. 55ff, 146ff.
[7] Th. Wolf, M.H. Pahl, Scale-Up-Kriterien für die Prallzerkleinerung, Aufbereitungstechnik 33 (10) (1992) 552–561.